JOURNAL OF GEOPHYSICAL RESEARCH, VOL. 98, NO. D10, PAGES 18,589–18,595, OCTOBER 20, 1993

Chaotic Advection in the Stratosphere: Implications for the Dispersal of Chemically Perturbed Air From the Polar Vortex

R. BRADLEY PIERCE

Atmospheric Sciences Division, NASA Langley Research Center, Hampton, Virginia

T. DUNCAN A. FAIRLIE

Science and Technology Corporation, Hampton, Virginia

The Lagrangian evolution of material lines within the northern hemisphere winter stratospheric vortex is determined using isentropic winds and diabatic heating rates obtained from the NASA Langley Research Center (LaRC) atmospheric circulation model. Transient, subtropical anticyclones lead to deformation of the material lines near the edge of the polar vortex which then rapidly evolve into elongated filaments as material is drawn around the anticyclones. The rate of stretching of the material lines is shown to be exponential, with typical *e*-folding times of the order of 4 to 8 days. These results provide evidence for "chaotic advection" near the edge of the stratospheric polar vortex which leads to rapid mixing of vortex air with tropical and midlatitude air. The characteristic timescales of these mixing processes and the extent to which the mixing penetrates the polar vortex have important implications for the dispersal of chemically perturbed air from the polar vortex throughout the northern hemisphere and attendant ozone depletion.

INTRODUCTION

The observed 2–6% reductions in middle- and high-latitude total ozone in the northern hemisphere stratosphere over the last 10 years [*Stolarski et al.*, 1991] have been linked to processing of stratospheric air within the polar vortex. An understanding of the processes that are responsible for the transport of processed air out of the vortex and subsequent mixing with midlatitude and subtropical air is fundamental to a complete understanding of the ozone depletion problem. A number of outstanding issues remain. What are the characteristic timescales for the dispersal of air from the polar vortex? How far into the polar vortex does the mixing process extend? To what extent does low-latitude air penetrate the vortex?

In this paper we address these issues by investigating the behavior of material lines located within the polar vortex in the lower stratosphere. We consider the behavior of material lines that are initially located on the 425 K surface of potential temperature (θ). Within the isentropic framework, θ is used as a vertical coordinate. Quasi-horizontal distortion of material lines which are initially located on isentropic surfaces is caused by transient adiabatic disturbances, while diabatic heating and cooling leads to vertical displacement of the material lines. The 425 K isentropic surface, which lies near 70 mbar in the lower stratosphere, corresponds to the region where the potential for chemical processing of stratospheric air and the attendant ozone losses are likely to be largest due to cold temperatures which favor the formation of polar stratospheric clouds (PSCs).

We have conducted numerical computations using full three-dimensional distributions of horizontal winds and radiative heating rates from the NASA Langley Research Center (LaRC) atmospheric circulation model [*Blackshear et al.*, 1987]. The stratospheric winds and heating rates are represented using spherical harmonic expansion in the horizontal (triangular truncation to wave number 16) and a vertical resolution of 3 km. The use of realistic large-scale stratospheric winds and radiative heating distributions in this investigation allows us to assess the impact of large-scale transport processes on the dispersal of polar air in the lower stratosphere.

Plate 1 shows streamlines of the circulation on the 425 K surface for December 1 of the LaRC model simulation. The map shows a large circumpolar cyclonic vortex with a counterclockwise circulation and smaller transient anticyclones which are located in subtropical latitudes. This pattern is fairly representative of the large-scale flow during midwinter in the lower stratosphere of the northern hemisphere, although the simulated vortex is considerably larger than is typically observed. The colored streamlines in Plate 1 reflect streamlines along which air parcels orbit within and around the edge of the polar vortex. During the model simulation the anticyclones move eastward around the polar vortex and the closed streamlines within the vortex deform, developing regions of increased curvature between the anticyclones. Rossby wave breaking [*McIntyre and Palmer*, 1983] may occur near such regions resulting in the ejection of filaments of vortex material into subtropical latitudes [*Polvani and Plumb*, 1992]. In this paper we will investigate the evolution and morphology of material lines which are initially coincident with the instantaneous streamlines within the polar vortex on December 1 of the model simulation.

LAGRANGIAN EVOLUTION OF VORTEX MATERIAL LINES

The differential advection of material elements by a three-dimensional, time-dependent circulation can be investigated by computing the Lagrangian evolution of a material line which is composed of an ensemble of parcels. The Lagrangian representation of three-dimensional advection of a material line composed of (n) parcels in isentropic coordi-

Paper number 93JD01619.
0148-0227/93/93JD-01619$05.00

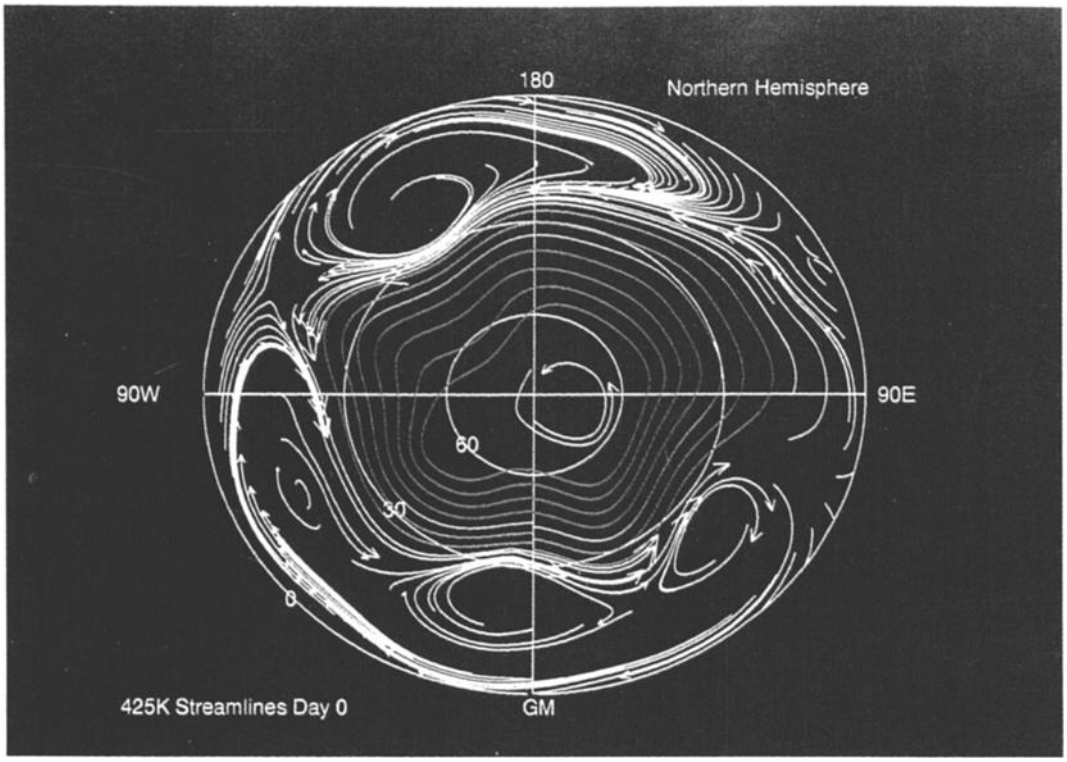

Plate 1. Polar stereographic plot of streamlines showing the northern hemisphere stratospheric circulation on the 425 K isentropic surface for December 1 of the LaRC model simulation. Arrows indicate the direction of the circulation. The closed lines within the interior of the circumpolar cyclonic vortex indicate the initial location of material lines which are coincident with the vortex streamlines.

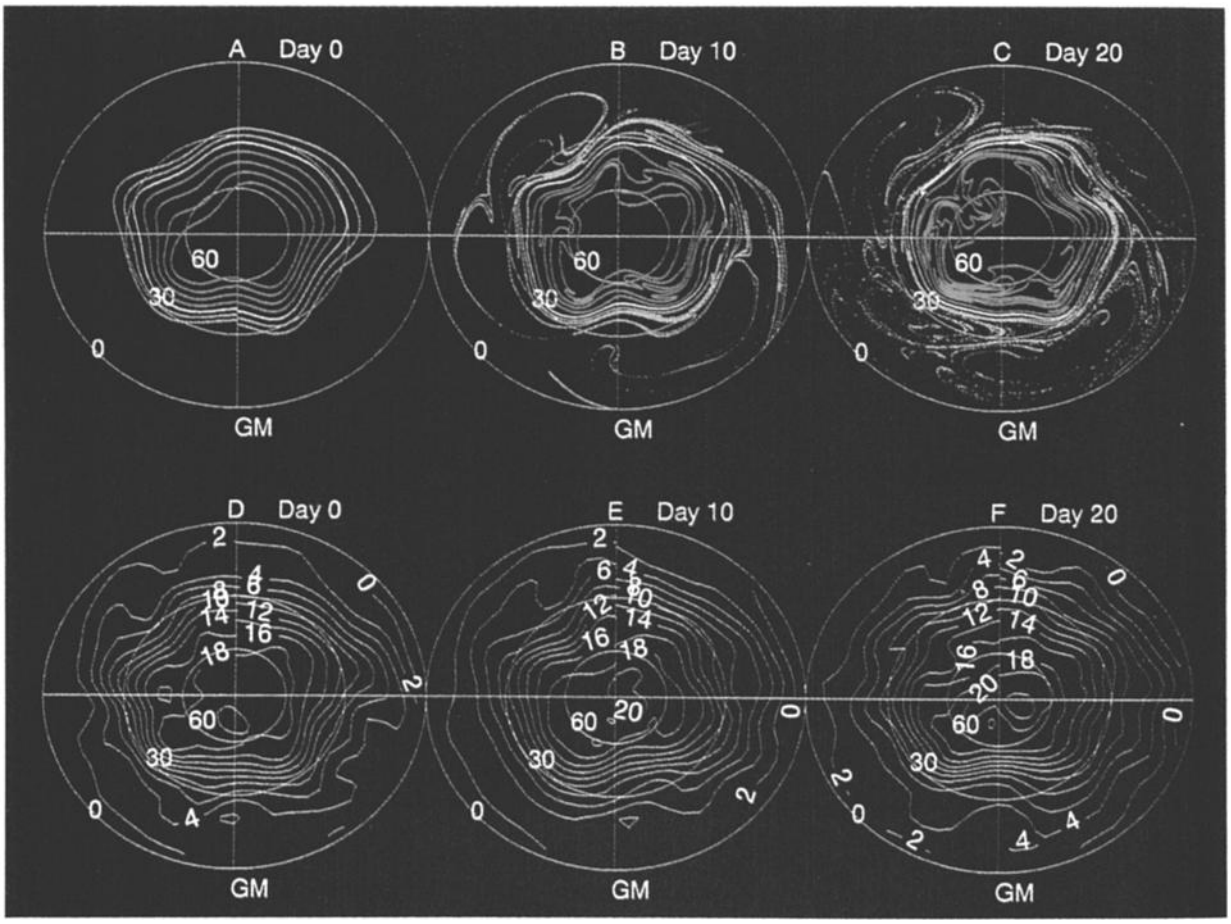

Plate 2. Polar stereographic plots of the horizontal projection of the material lines during the Lagrangian integration for (*a*) day 0, (*b*) day 10, and (*c*) day 20. Colors indicate the flow regime of the material lines; red denotes interior material lines, white the separating material line, and yellow the edge material lines. The 425 K potential vorticity distributions are shown in the bottom panels for (*d*) day 0, (*e*) day 10, and (*f*) day 20. Contour intervals are 1×10^{-6} K m^2 s^{-1} kg^{-1}

nates is equivalent to the simultaneous solution of $3n$ ordinary differential equations

$$\dot{x}_i = u(x_i, y_i, \theta_i, t),\ i = 1, n \quad (1a)$$

$$\dot{y}_i = v(x_i, y_i, \theta_i, t),\ i = 1, n \quad (1b)$$

$$\dot{\theta}_i = Q(x_i, y_i, \theta_i, t),\ i = 1, n \quad (1c)$$

where u and v are the x and y components of the velocity field evaluated on an isentropic surface θ and Q is the diabatic heating rate associated with departures of the stratospheric temperatures from radiative equilibrium values. The numerical calculations of the Lagrangian evolution of vortex material lines involve quasi-isentropic trajectory computations performed in an off-line mode [*Mahlman and Moxim*, 1978]. Winds and diabatic heating rates from the LaRC atmospheric circulation model are stored at 3-hour increments for the trajectory calculations. An implicit integration scheme [*Austin and Tuck*, 1985] was used to integrate equations (1*a*)–(1*c*), with winds and heating rates which are linearly interpolated in time.

Different techniques have been developed for Lagrangian material line simulations. A "contour surgery" technique was developed by *Dritschel* [1988] for use in contour dynamics. Contour surgery involves the continual adjustment of the number of parcels used to define the material line. *Waugh and Plumb* [1993] have shown that contour surgery accurately predicts the evolution of material lines for a variety of modeled and observed stratospheric flows. This technique has also been used by *Norton* [1993] in shallow water simulations. Here, we chose a different approach. We initialize the material lines with a sufficiently large number of parcels to accurately predict the evolution of the material lines over the period we are simulating. For these experiments, over 150,000 individual parcel trajectories were computed for a period of 20 days. The initial density of the ensemble of parcels along the instantaneous streamline determines the length of time that the deformation of the material line can be accurately computed. This technique is not as computationally efficient as contour surgery, although it does provide a means of accurately resolving the initial development of vortex filaments, which begin as small-scale folds in the material lines.

Plate 2 shows the evolution of the vortex material lines during the 20-day integration. Plates 2*a*–2*c* depict the horizontal distribution of the material lines for days 0, 10, and 20 of the Lagrangian simulation. Plates 2*d*–2*f* show the distribution of potential vorticity (PV) on the 425 K surface for these days. By day 10, material lines near the edge of the polar vortex (yellow material lines) have developed long filaments extending from the vortex edge into the tropics. Material lines in the interior of the polar vortex (red material lines) have a very different morphology. These material lines typically develop intrusions which extend poleward, then fold onto themselves. The white material line deforms in a quasi-periodic manner with very little net change throughout the 20-day simulation. This material line separates two regions of distinctly different Lagrangian behavior. This material line will be referred to as the separating material line.

Within the vortex, material lines characteristically develop multiple folds with minimal stretching. Near the vortex edge, parts of the material lines remain associated with the polar vortex and other parts of the material lines stretch into long filaments leading to the dispersal of air throughout tropical and subtropical latitudes. The development of filamentary structures near the edge of the polar vortex by large-scale advective processes is likely to enhance the efficiency of small-scale mixing of vortex edge air with tropical and midlatitude air by increasing the interfacial surface area of the boundary between these air masses. The large-scale features of the material lines are evident in the computed potential vorticity distributions (Plates 2*d*–2*f*). The white material line, which separates the two regions in the Lagrangian simulation, lies near the largest meridional gradients in PV. The PV distribution shows evidence of the folding behavior found for the interior material lines near 225° on day 20. There is no evidence of the long filaments which characterize the material lines at the edge of the vortex.

Plates 3*a*–3*c* show meridional projections of the material lines for days 0, 10, and 20 of the Lagrangian simulation. The material lines are initialized on the 425 K surface. However, as the Lagrangian simulation proceeds, the material lines are displaced in the vertical due to diabatic processes which result in cross isentropic movement of air parcels. The vertical displacement of the material lines during the simulation is small since the 425 K isentropic surface is well below the level of maximum radiative heating in the middle stratosphere. However, there is a systematic latitudinal difference between the vertical displacement of the material lines. Radiative cooling due to CO_2 emission leads to a slow descent of the material lines within the interior of the vortex. The largest diabatic descent occurs near 45°N due to enhanced radiative cooling of adiabatically warmed air parcels in the region between the vortex and the transient anticyclones. The separating material line lies within this region of strongest diabatic descent. Subtropical latitudes are sunlit during early and mid-December. Ultraviolet absorption by ozone leads to weak radiative heating in these latitudes which results in the very slow ascent of the vortex filaments as they extend into tropical latitudes. Radiative cooling rates near the edge of the vortex during the Lagrangian simulation range from 1° to 2°K per day. Significantly larger local cooling rates (5–10 K per day) associated with high, cold cirrus clouds have been found near the edge of the polar vortex [*Tuck et al.*, 1992]. In the real atmosphere, local diabatic descent associated with these cloud decks may significantly affect the Lagrangian behavior of the vortex filaments.

CHARACTERISTIC TIMESCALES OF THE MATERIAL LINE DEFORMATION

The system defined by equations (1*a*)–(1*c*) is formally equivalent to a nonautonomous dynamical system and lends itself naturally to the application of the concepts of dynamical systems theory. The mathematical similarity between the Lagrangian evolution equations and the nonautonomous dynamical systems introduces the possibility of chaotic parcel trajectories. *Aref* [1984] investigated the Lagrangian evolution of an ensemble of parcels in a two-dimensional ($Q = 0$), incompressible, laminar flow. He found that the parcel motion was stochastic and termed this stochastic response to deterministic flow "chaotic advection." *Khakhar et al.* [1986] have shown that the presence of chaotic advection is

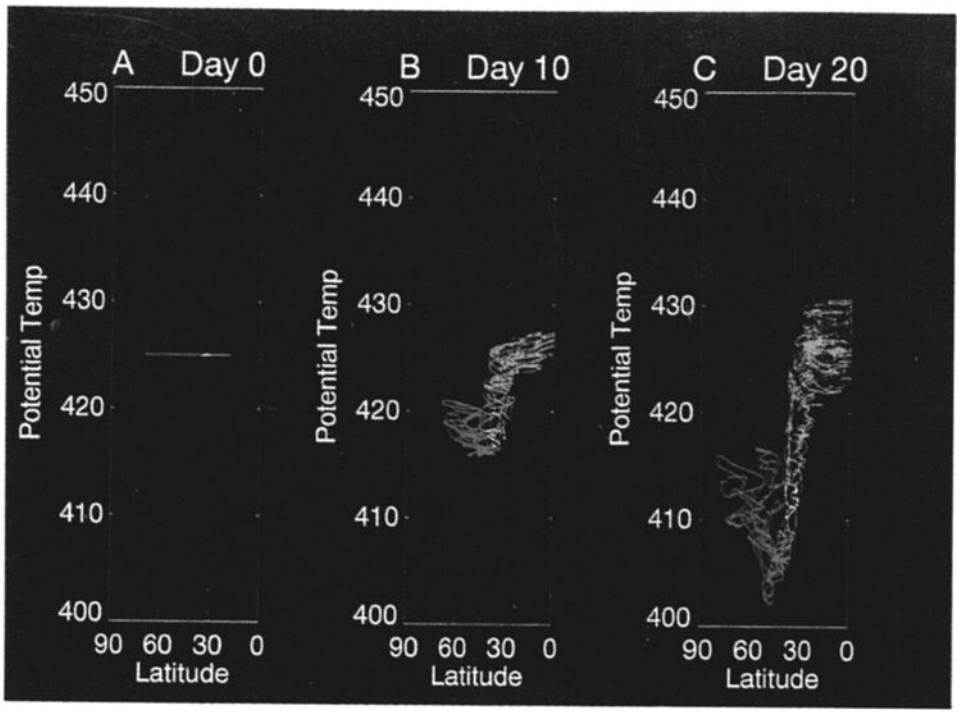

Plate 3. Meridional projections of the material lines during the Lagrangian integration for (*a*) day 0, (*b*) day 10, and (*c*) day 20.

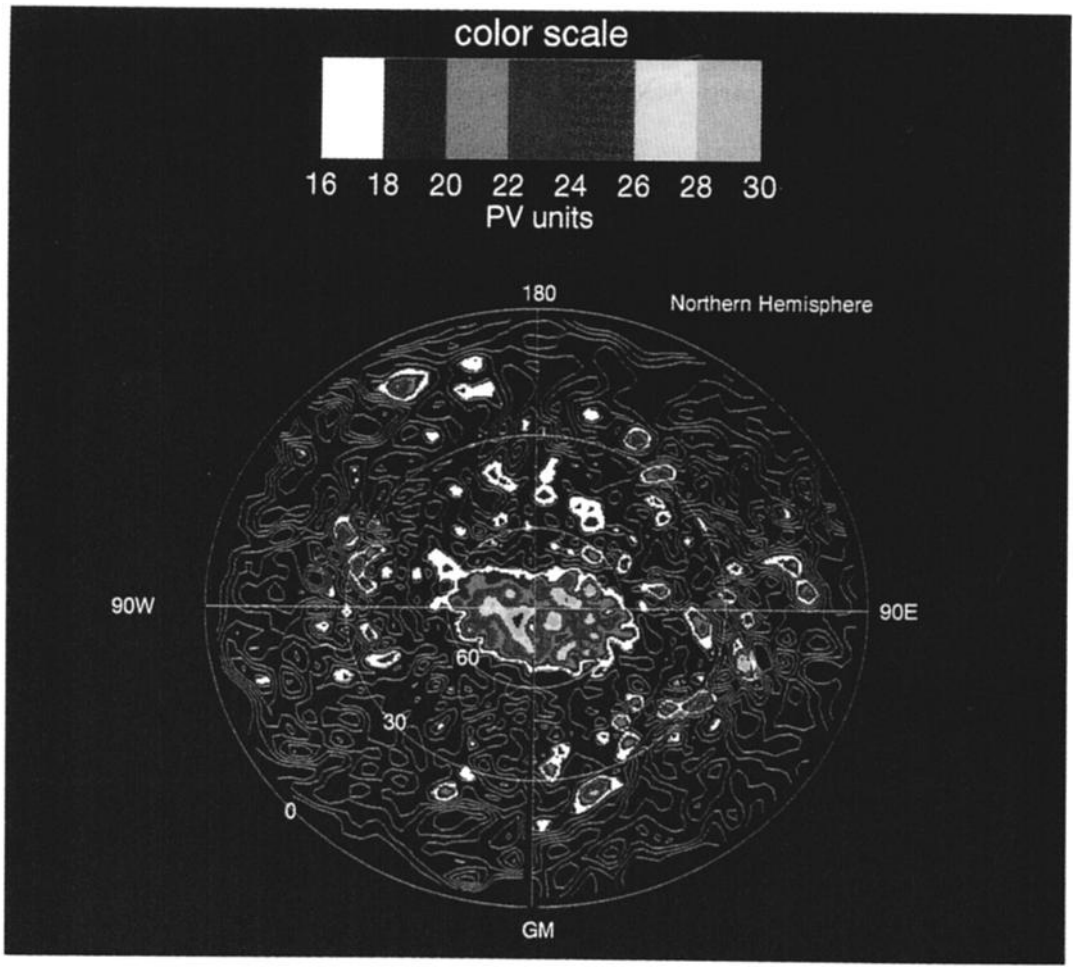

Plate 4. Polar stereographic plot of isentropic potential vorticity for December 24, 1988, on the 425 K isentropic surface. Potential vorticity data were provided by Terry Davies and were obtained from European Centre for Medium Range Weather Forecasting (ECMWF) operational analyses. Potential vorticity greater than 16 isentropic potential vorticity (IPV) units is considered "vortex debris" and is shaded. Potential vorticity less than 16 IPV units is contoured with an interval of three potential vorticity (PV) units.

related to the efficiency of mixing processes. In their simulations, simple time-dependent flows were able to deform material lines to scales which were much smaller than the length scale of the flow itself, thereby leading to efficient mixing. The material lines were found to stretch at an exponential rate in the regions of the flow where chaotic advection was occurring. Liapunov exponents provide an invariant measure of the characteristic timescales of a dynamical system. For chaotic advection the Liapunov exponent is directly related to the long-time average of the "specific stretching rate" of material lines [*Khakhar et al.*, 1986]. If material lines deform at an exponential rate, then the rate constant of the deformation is equal to the specific stretching rate of the material lines.

We monitored the length of the vortex material lines over the 20-day simulation to determine whether chaotic advection was occurring in the Lagrangian simulation of the vortex material line deformation. Figure 1 shows the computed length of the material lines normalized by their initial lengths as a function of time. Material lines are designated by numbers which increase with the distance from the vortex center. Linear and exponential best fits to the computed curves are also shown. Material lines 1–4 (red in Plate 2) stretch by 2 to 4 times their initial length over the 20-day simulation. Material lines 6 and 7 (yellow in Figure 2) stretch from 1 and 2 orders of magnitude during the simulation. The separating material line is number 5 and does not show any net stretching during the 20-day simulation. Root-mean-square (rms) errors for linear and exponential least squares fits to the curves indicate that the stretching rate of the two material lines closest to the edge of the vortex (material lines 6 and 7) are best characterized as exponential. The rms errors in linear and exponential least squares fits for the interior material lines (material lines 1–4) are so close that both provide a good fit, although the exponential rate constant is quite small. The separating material line lies between the linear and the exponential stretching rate regions.

The evolution of material lines in the neighborhood of the separating material line is likely to be quite sensitive to the initial location of the material line. An additional simulation was performed to examine this sensitivity. Six material lines, three on each side of the separating material line at 1° latitudinal increments, were initialized to investigate the characteristics of the transition zone between linear and exponential stretching rate regimes. The three material lines which were poleward of the separating material line showed no net stretching initially but then began stretching near day 15 as the material lines began folding in on themselves. The three material lines which were equatorward of the separating material line showed more stretching, extending equatorward within the envelope formed by material lines 5 and 6. The material line which was initialized 3° equatorward of the separating material line stretched 5 times its initial length and extended well into the tropics by day 20.

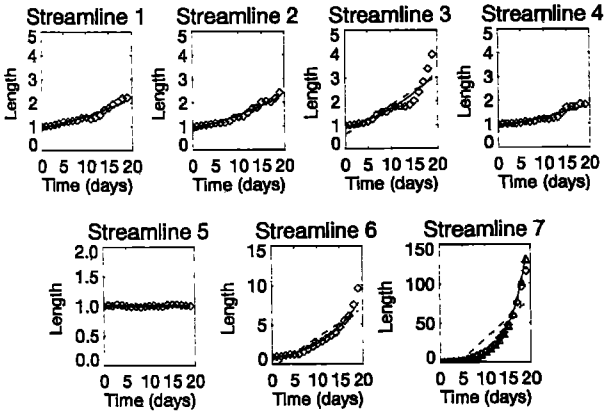

Fig. 1. Computed length of the material lines versus time during the Lagrangian integration. Streamlines are numbered from the interior of the vortex outward. Squares indicate the computed length of the material line. The solid lines indicate the least squares best fit to the data assuming an exponential stretching rate. The dashed lines indicate the least squares best fit to the data assuming a linear stretching rate. The lengths are normalized by the initial length of the material lines.

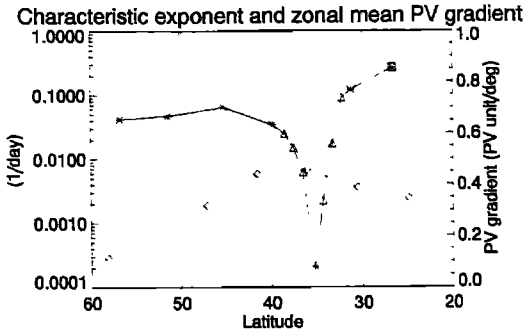

Fig. 2. The characteristic timescales for the material line deformation during the Lagrangian simulation (solid line) computed from the *e*-folding times of the least squares exponential fits of the material line deformation shown in Plate 3. The meridional gradient of the initial zonal mean potential vorticity is also shown (dashed line). Characteristic timescales are related to latitude by the initial mean location of the material lines. The zonal mean potential vorticity is computed at the Gaussian latitude points of the LaRC model.

The accuracy of our stretching rate calculations in the region which is characterized by exponential stretching rates was also investigated with a high-resolution Lagrangian simulation. We initialized a high-resolution material line on material line 7 which had the largest stretching rate in the original simulation. The initial parcel density of this new material line was 10 times greater than in the original simulation. The deformation rate of the high-resolution material line was virtually identical to the original material line. The computed *e*-folding times differed by less than 1% which indicates that we have initialized a sufficient number of parcels to adequately describe the material line deformation during this period.

Figure 2 shows the characteristic exponents of the original seven material lines (stars), material lines in the neighborhood of the separating material line (triangles), and high-resolution material line (square) plotted as a function of the initial mean latitude of the material lines. The exponents characterize the deformation rate of the material lines and are determined from the least squares exponential fit to the material line deformation (cf. Figure 1). The characteristic exponent is equal to the time-averaged specific stretching rate of the material lines and therefore provides a crude estimate of the Liapunov exponent which characterizes the Lagrangian behavior of the material lines. The zonal mean potential vorticity gradient on the 425 K surface is also

shown. The maximum gradient in potential vorticity, which is generally coincident with the zonal jet maximum and is often used to define the edge of the polar vortex, is located near 40°N. The maximum PV gradient is typically observed near 60°N at this level in the Arctic stratosphere [*Tuck et al.*, 1992]. The difference reflects an inability of the LaRC model to adequately represent the polar night jet in the lower stratosphere.

The characteristic timescale of the material lines outside the vortex is of the order of 4 to 8 days. Within the vortex (north of 40°N) the characteristic timescale is of the order of 15 to 30 days. Between these regimes lies a narrow zone approximately 5° wide with much longer characteristic timescales. This zone acts as an effective barrier to large-scale horizontal transport of material from within the vortex during the simulation. Similar zones have been found in idealized models of chaotic mixing [*Khakar et al.*, 1986; *Behringer et al.*, 1991]. In two-dimensional flows they are composed of "KAM curves" [*Guckenheimer and Holmes*, 1983] which enclose an "island" of fluid with regular, quasi-periodic behavior that does not mix with the surrounding fluid. The length of time that an island of fluid remains isolated is determined by the survival of the outermost KAM curves. In the stratosphere the survival of the separating material line is sensitive to the amplitude of the transient waves and to the frequency of rotation of the trajectories about the polar vortex. It is likely that the separating material line would eventually succumb to changes in the shear deformation and begin stretching. The evolution of the material lines in the neighborhood of the separating material line supports this hypothesis.

These calculations establish that positive Liapunov exponents exist for the stratospheric circulation. Unfortunately, a robust quantitative estimate of the Liapunov exponent cannot be obtained using these techniques due to the relatively short period of time over which the averaging occurs. Long-term Lagrangian simulations are not feasible because of numerical errors in the computation of the individual parcel trajectories which also grow at an exponential rate in the regions of chaotic advection [*Franjione and Ottino*, 1987]. However, the existence of positive Liapunov exponents indicates that chaotic advection is occurring near the edge of the polar vortex in this model simulation of the northern hemisphere lower stratosphere. The chaotic advection is characterized by the development of filaments of vortex material which extend well into the tropics on timescales of 4 to 8 days.

DISCUSSION

Our simulations indicate that a significant amount of the air near the edge of the polar vortex may be drawn into thin filaments through chaotic advective processes. The development of filamentary structures in constituent distributions can drastically increase the efficiency of mixing by increasing the interfacial surface area between different air masses. *Prather and Jaffe* [1990] investigated the impact of stretching, molecular diffusion, and photochemistry on chemically perturbed air parcels embedded in a homogeneously turbulent circulation. They found that the evolution of chemically perturbed air parcels in the lower stratosphere was controlled by stretching until scales became small enough for molecular diffusion to become important. They predicted that chemically perturbed air parcels would remain isolated for 7–20 days assuming a random strain rate of 10^{-5} s^{-1}. They noted that the primary uncertainty in their calculations is the strain rate used in their model. For homogeneous turbulence the specific stretching rate of a material line is equal to the Lagrangian-averaged strain rate of the flow [*Batchelor*, 1952]. The computed specific stretching rates due to chaotic advection suggest that the actual strain rate near the outer edge of the vortex is of the order of 2×10^{-6} s^{-1}, which would result in even longer isolation times. The dominance of stretching over diffusive and photochemical processes in determining the evolution of exvortex air masses indicates that chaotic advection could have a significant impact on the distribution of trace constituents in the lower stratosphere.

Our simulations also suggest that the large-scale horizontal exchange of vortex material is restricted by a zone near the edge of the vortex which acts as an effective barrier to large-scale mixing. We are left with an apparent dichotomy. Material slightly poleward of the separating material line is highly isolated from the surrounding circulation, yet material slightly equatorward of the separating material line mixes very effectively with the middle latitude and tropical air masses. High-resolution assimilated stratospheric data sets may provide insight into the effectiveness of this barrier in the real atmosphere.

Plate 4 shows a map of isentropic potential vorticity (IPV) on the 425 K isentropic surface for December 24, 1988, just prior to the first Airborne Arctic Stratospheric Expedition (AASE). The IPV map was provided by Terry Davies of the European Centre for Medium Range Weather Forecasting (ECMWF) and was produced at a triangular 63 spectral resolution. High values of IPV, which are typical of vortex air, are dispersed throughout middle and subtropical latitudes. Large amounts of such "vortex debris" were found in ECMWF IPV analysis throughout the AASE mission [*Tuck et al.*, 1992]. The interpretation of these small-scale features in stratospheric IPV analyses is admittedly plagued with uncertainties. If one assumes that the vortex debris reflects the signature of the vortex filaments, then clearly there is a significant potential for aliasing of these narrow features. In a spectral model this aliasing could result in the bloblike appearance and lack of continuity which is often associated with the small-scale features in the IPV distribution. Alternatively, the small-scale features may reflect the impact of noise generated during the assimilation process. In spite of these uncertainties the assimilated IPV distributions provide us with a dynamically consistent depiction of the quasi-horizontal transport in the lower stratosphere. The relatively high potential vorticity values of some of the debris indicates that this air came from well within the polar vortex. The presence of air with potential vorticity characteristic of the interior of the vortex suggests that exchange processes other than large-scale chaotic advection play an important role near the vortex edge.

Danielsen et al. [1991] have shown that cross-jet transport of trace constituents in the lower stratosphere is dominated by low-frequency inertial-gravity waves. Quasi-isentropic transport by these small-scale waves leads to pronounced laminae in the vertical distribution of ozone near the northern hemisphere polar vortex edge [*Danielson et al.*, 1991; *Reid and Vaughhan*, 1991; *Browell et al.*, 1990]. The large amounts of relatively high potential vorticity air outside of

the polar vortex may reflect transport across the polar jet by small-scale inertia-gravity waves, followed by dispersal of the vortex air by large-scale chaotic advection. The importance of the coupling between these two disparate scales of motion near the vortex boundary needs further investigation.

REFERENCES

Aref, H., Stirring by chaotic advection, *J. Fluid Mech.*, *143*, 1–21, 1984.

Austin, J., and A. F. Tuck, The calculation of stratospheric air parcel trajectories using satellite data, *Q. J. R. Meteorol. Soc.*, *111*, 279–307, 1985.

Batchelor, G. K., The effects of homogeneous turbulence on material and line surfaces, *Proc. R. Soc. London, Ser. A*, *213*, 349–366, 1952.

Behringer, R. P., S. D. Meyers, and H. L. Swinney, Chaos and mixing in a geostrophic flow, *Phys. Fluids, Ser. A*, *3*, 1243–1249, 1991.

Blackshear, W. T., W. L. Grose, and R. E. Turner, Simulated sudden stratospheric warming; synoptic evolution, *Q. J. R. Meteorol. Soc.*, *113*, 815–846, 1987.

Browell, E. V., et al., Airborne lidar observation in the wintertime Arctic stratosphere: Ozone, *Geophys. Res. Lett.*, *17*, 325–328, 1990.

Danielsen, E. F., R. S. Hipskind, W. L. Starr, J. F. Vedder, S. E. Gaines, D. Kley, and K. K. Kelly, Irreversible transport in the stratosphere by internal waves of short vertical wavelength, *J. Geophys. Res.*, *96*, D9, 17,433–17,452, 1991.

Dritschel, D. G., Contour surgery: A topological reconnection scheme for extended integrations using contour dynamics, *J. Comput. Phys.*, *77*, 240–266, 1988.

Franjione, J. G., and Ottino, Feasibility of numerical tracking of material lines and surfaces in chaotic flows, *Phys. Fluids*, *30*, 3641–3643, 1987.

Guckenheimer, J., and P. Holmes, *Non-Linear Oscillations, Dynamical Systems, and Bifurcation of Vector Fields*, Springer-Verlag, New York, 1983.

Khakhar, D. V., H. Rising, and J. M. Ottino, Analysis of chaotic mixing in two model systems, *J. Fluid Mech.*, *172*, 419–451, 1986.

Mahlman, J. D., and W. J. Moxim, Tracer simulation using a global general circulation model: Results for a midlatitude instantaneous source experiment, *J. Atmos. Sci.*, *35*, 1340–1374, 1978.

McIntyre, M. E., and T. N. Palmer, Breaking planetary waves in the stratosphere, *Nature*, *305*, 593–600, 1983.

Norton, W. A., Breaking Rossby waves in a model stratosphere diagnosed by a vortex-following coordinate system and a technique for advecting material contours, *J. Atmos. Sci.*, in press, 1993.

Polvani, L. M., and R. A. Plumb, Rossby wave breaking, microbreaking, filamentation, and secondary vortex formation: The dynamics of a perturbed vortex, *J. Atmos. Sci.*, *49*, 462–476, 1992.

Prather, M., and A. H. Jaffe, Global impact of the Antarctic ozone hole: Chemical propagation, *J. Geophys. Res.*, *95*, 3473–3492, 1990.

Reid, S. J., and G. Vaughan, Lamination in ozone profiles in the lower stratosphere, *Q. J. R. Meteorol. Soc.*, *117*, 825–844, 1991.

Stolarski, R. S., P. Bloomfield, R. D. McPeters, and J. R. Herman, Total ozone trends deduced from Nimbus 7 TOMS data, *Geophys. Res. Lett.*, *18*, 1015–1018, 1991.

Tuck, A. F., et al., Polar stratospheric cloud-processed air and potential vorticity in the northern hemisphere lower stratosphere at midlatitudes during winter, *J. Geophys. Res.*, *97*, 7883–7904, 1992.

Waugh, D. W., and R. A. Plumb, Contour advection with surgery: A technique for investigating fine-scale structure in tracer transport, *J. Atmos. Sci.*, in press, 1993.

T. D. A. Fairlie, Science and Technology Corporation, Hampton, VA 23666.

R. B. Pierce, Atmospheric Sciences Division, NASA Langley Research Center, Hampton, VA 23681-0001.

(Received January 5, 1993;
revised June 8, 1993;
accepted June 9, 1993.)